Asymmetric responses of microbial community structure mediated by root exudates under grazing

wei wen

184347663030163.com

Inner Mongolia University

Research Article

Keywords: Short-term and Long-term grazing, Root exudates, Structure of the microbial community, Gibbs free energy of oxidation, molecular structural complexity

Posted Date: August 6th, 2026

DOI: https://doi.org/10.21203/rs.3.rs-10600404/v1

Additional Declarations: The authors declare no competing interests.

Abstract

Grazing alters the interactions between plants and microbial and has a significant impact on grassland ecosystems, with root exudates (RE) serving as the primary mechanism by which plants regulate and maintain microbial communities. However, little is known about how RE regulate microbial communities under grazing stress, or whether the efficacy of key metabolites is limited by their thermodynamic properties or molecular structure. By analyzing RE metabolites, rhizosphere microbial communities, and the physicochemical properties of rhizosphere soil in typical grassland in Inner Mongolia, China, we found that: (1) short-term grazing exerted a stronger effect on RE metabolites of *Stipa grandis*. RE metabolites explained significantly more variation in rhizosphere microbial communities than soil physicochemical properties, and showed deeper coupling with rhizosphere fungal communities; (2) the abundance of RE metabolites varied with grazing duration and intensity. Under short-term grazing pressure, *S. grandis* upregulated energy-rich lipids and specific signaling molecules (e.g., (-)-jasmonic acid) to drive rapid bacterial growth. In contrast, under long-term moderate grazing, plants shifted toward sustained secretion of defensive secondary metabolites, maintaining mutually beneficial associations with rhizosphere fungi; (3) under resource-limited conditions induced by long-term moderate grazing, the topological position of key RE metabolites in bacteria-associated networks were constrained by thermodynamic properties, whereas their position in fungi-associated networks was generally constrained by molecular structural complexity across multiple grazing treatments. These findings fill a critical knowledge gap in grassland ecosystem research and provide an important theoretical basis, from a microbiological perspective, for enhancing grassland productivity and the restoration of degraded grasslands more broadly.

Introduction

Grazing is one of the dominant anthropogenic disturbances in temperate grassland ecosystems, influencing biogeochemical cycling by altering community structure and resource allocation (Ren et al., 2024; Gao et al., 2025). In natural environments, plants do not exist in isolation; their nutrient acquisition, growth, and adaptation largely depend on soil microbes (Qiao et al., 2024). The rhizosphere serves as a key interface for material exchange and information transfer between plants and soil, where resident microbial communities are widely regarded as the plant's "second genome" and play central roles in nutrient cycling, stress tolerance, and ecological adaptation (Mendes et al., 2011; Qiao et al., 2024). Thus, in grassland ecosystems, elucidating plant–microbe interactions under grazing disturbance are crucial for understanding their ecological response mechanisms.

Plants secrete approximately 20–40% of photosynthetically fixed carbon (C) into the rhizosphere in the form of compounds (Bölscher et al., 2025). These root exudates (RE) not only provide substrates for microbial growth but also mediate the exchange of matter and information between plants and microbes through signaling molecules, thereby regulating the structure and function of rhizosphere microbial communities and indirectly enhancing plant stress tolerance and productivity (Sasse et al., 2018). In addition, RE play central biochemical roles in mobilizing insoluble soil nutrients, such as phosphorus, and

mediating allelopathic interactions among plants (Ding et al., 2025; Ji et al., 2025). In grassland ecosystems, studies have shown that in long-term warmed temperate grasslands, the effects of RE on microbial communities are species-specific (Yu et al., 2026), whereas in grazed grasslands, grazing significantly alters the allocation of photosynthetic C to belowground tissues (Wilson et al., 2018), with RE rates increasing with grazing intensity (Shen et al., 2020). Despite the multiple roles of RE in grassland ecosystems, their regulatory effects on microbial communities under grazing remain poorly understood, which substantially limits our understanding of grassland ecosystem processes and stability.

Although extensive reports that grazing alters soil microbial community composition in grasslands (Guo et al., 2025), it remains unclear whether RE act as key drivers of these changes, particularly across different grazing time scales. More importantly, differences in physiological traits and evolutionary histories between bacteria and fungi may lead to asymmetric responses to plant metabolite-mediated strategies (Wang and Kuzyakov, 2024). Typically, copiotrophic bacteria exhibit relatively fast growth rates and are more sensitive to fluctuations in small-molecule substrates such as carbohydrates and organic acids (Chen et al., 2021). In contrast, fungi, with their extensive hyphal networks and extracellular enzyme systems, display greater tolerance under conditions of complex substrate decomposition and resource limitation (Coleine et al., 2022). Under continuous grazing disturbance, such niche differentiation may be further amplified. Previous studies have shown that soil fungal communities often maintain relatively high stability under intense grazing pressure (Che et al., 2019). However, it remains largely untested whether RE of plant play a role in this relatively conservative community response.

Under prolonged grazing pressure, the persistent decline in aboveground biomass severely limits plant C fixation (Liu et al., 2024). Maintain cross-kingdom communication mediated by RE, plants may need to balance energetic expenditure and signaling efficiency under resource-limited conditions (Badri and Vivanco, 2009). The underlying biochemical rules governing this adaptive trade-off remain largely unexplored. From a structural and thermodynamic perspective, the Gibbs free energy of oxidation (ΔG_{ox}) and molecular structural complexity of metabolites determine their synthesis cost, degradability, and bioavailability (Wang and Kuzyakov, 2024; Sun et al., 2025). Under extreme grazing pressure, it remains unclear whether molecular structural complexity and thermodynamic properties constrain metabolite utilization efficiency and thereby reflect adaptive trade-offs in plant mediated cross kingdom communication, and this aspect remains largely unexplored (Yang et al., 2026).

To address these questions, this study leveraged long-term and short-term grazing (LTG and STG) experimental platforms in a typical Inner Mongolian grassland, using the dominant species *Stipa grandis* as the study system. RE and their corresponding rhizosphere soils were collected in situ under different grazing durations and intensities. By combining untargeted metabolomics with amplicon sequencing, and innovatively applying the iCAMP framework, complex metabolites were grouped into “phylogenetic bins” based on molecular structural similarity. Using this binning strategy, we identified key metabolites and further explored their potential impacts on microbial communities and the adaptive trade-offs in cross-kingdom communication. We hypothesize that: 1) compared with LTG, STG, as the initial phase of

disturbance, has a stronger effect on the metabolites of *S. grandis* RE; 2) changes in RE metabolites are a primary driver of rhizosphere microbial community dynamics, exhibiting asymmetric effects on bacteria and fungi; and 3) Under resource-limited conditions, cross-kingdom communication mediated by root exudates is constrained by the thermodynamic properties and molecular structural complexity of metabolites. This study aims to provide a biochemical and thermodynamic perspective on cross-kingdom communication between plants and microbes, which is mediated by RE under grazing disturbance in grassland ecosystems, thereby offering a theoretical basis for optimizing grazing management and improving grassland sustainability.

Materials and methods

Study site and experiment design

This study was conducted at the Grassland Ecosystem Research Station of Inner Mongolia University, located approximately 60 km northeast of Xilinhot City (116°31'18"–116°32'28" E, 44°15'24"–44°15'41" N; 1146 m a.s.l.). The region features a temperate semi-arid climate with a mean annual temperature of 2.7°C and precipitation of 284 mm. The typical steppe vegetation is dominated by *S. grandis* and *Leymus chinensis*. The predominant soil is a sandy-loam shallow chestnut soil, classified as a Calcic-humic Aridisol according to the USDA system (Wang et al., 2020). The grazing platform was established in a flat typical steppe fenced since 2012. LTG (established 2017) and STG (established 2023) experiments were situated in adjacent areas with identical designs. A randomized block design utilized twelve 0.25 hm^2 (50 m × 50 m) paddocks under nil, light, and moderate grazing, with stocking rates of 0, 3, and 9 sheep per paddock, respectively.

Sampling was conducted in July 2024, when aboveground biomass reaches its annual peak and immediately after the grazing period (Li et al., 2025). At this time, LTG and STG had been maintained for 8 and 2 years, respectively. Five grazing treatments were included, namely nil (NG), short-term light (SLG), short-term moderate (SMG), long-term light (LLG), and long-term moderate (LMG). Three replicate blocks were selected per treatment, with two samples collected per block. For RE metabolomics analysis, each sample pooled exudates from six randomly selected *S. grandis* plants. In total, RE and corresponding rhizosphere soils from 180 *S. grandis* plants were collected, yielding 30 effective sample sets for subsequent analyses.

Soil Sampling and analysis

Simultaneously with the collection of RE, the corresponding rhizosphere soil of *S. grandis* was harvested. Twelve plants were randomly selected within each replicate block; after gently shaking off the loose bulk soil, the soil tightly adhering to the root surfaces was collected using a soft brush. The rhizosphere soil from every six plants was pooled into a composite sample. Each soil sample was divided into three portions for respective preservation and analysis. The first fresh portion was immediately frozen in liquid

nitrogen for microbial community sequencing. The second fresh portion was stored at 4°C to determine moisture content (MC), dissolved organic carbon (DOC), ammonium nitrogen (NH_4^+), nitrate nitrogen (NO_3^-), microbial biomass carbon (MBC), microbial biomass nitrogen (MBN), and the activities of sucrase (SC), urease (UE), cellulase (CL), dehydrogenase (DHA), and alkaline phosphatase (AKP). The third portion was air-dried at room temperature for the determination of total carbon (TC), total nitrogen (TN), total phosphorus (TP), and available phosphorus (AP).

Root exudate collection and analysis

The collection of RE was adapted from the method of Phillips et al. *S. grandis* plants representing the overall post-grazing condition of each plot were selected for sampling (Phillips et al., 2008). Fine roots connected to the root base within the 0–20 cm soil layer were carefully excavated and gently rinsed with deionized water to remove adhering soil. The intact, soil-free fine roots were then placed in a collection device containing acid-washed coarse silica sand to simulate soil mechanical pressure. Deionized water was introduced into the device via a silicone tube connected to a syringe, and the device was positioned at a 45° angle to maintain the roots in *situ*. After 24 hours, the deionized water in the device was withdrawn and replaced five times to ensure residual exudates were removed, and fresh deionized water was then added for formal collection. After another 24 hours, the water containing RE was withdrawn using a vacuum pump, rinsed five times, and collected as the exudate solution. The solution was then concentrated using a rotary evaporator under near-vacuum conditions at 30°C to remove the majority of the water. Finally, the concentrated solution was lyophilized under vacuum to obtain dry root exudate powder, which was subsequently used for metabolomic analysis.

The lyophilized RE were reconstituted in a methanol/water mixture (4:1, v/v) containing 0.02 mg/mL L-2-chlorophenylalanine as an internal standard. After vortexing and brief sonication, the samples were centrifuged at 13,000 × g for 15 min at 4°C, and the supernatant was transferred to vials for analysis. LC-MS/MS analysis was performed using a UPLC-Triple TOF 5600 system (AB SCIEX) equipped with an HSS T3 column (100 mm × 2.1 mm, 1.8 μm) in both positive and negative ion modes. Raw mass spectra were processed using Progenesis QI (Waters Corporation, Milford, USA) software for baseline filtering, peak picking, retention time alignment, and peak matching. Metabolites were annotated using the HMDB (http://www.hmdb.ca/) and Metlin (https://metlin.scripps.edu/) databases. Following data preprocessing, partial least squares discriminant analysis (PLS-DA) was conducted using the R package "ropls". Differential metabolites were identified based on a variable importance in projection (VIP) > 1 and $P < 0.05$. Finally, pathway annotation for the specified metabolite bins was performed using the KEGG database (https://www.kegg.jp/kegg/pathway.html), and enrichment analysis was conducted utilizing the Python package "scipy.stats".

Sequence processing and microbial community analysis

Total genomic DNA was extracted from the rhizosphere soils of *S. grandis* using the E.Z.N.A.® Soil DNA Kit (Omega Bio-tek, Norcross, GA, USA). The V3–V4 region of the bacterial 16S rRNA gene and the fungal ITS1 region were amplified using the universal primer pairs 338F/806R and ITS1F/ITS2R, respectively. PCR products were purified and quantified, and sequencing libraries were constructed using the NEXTFLEX Rapid DNA-Seq Kit. Paired-end high-throughput sequencing was performed on the Illumina NextSeq 2000 platform. Raw sequences were quality-filtered using fastp (v0.19.6) and paired-end reads were merged with FLASH (v1.2.11). The resulting sequences were denoised using the DADA2 plugin in the QIIME2 pipeline to generate amplicon sequence variants (ASVs). Taxonomic classification of bacterial and fungal ASVs was performed using the SILVA database (v138.2) and the UNITE database (v10.0), respectively, with a Naive Bayes classifier. Sequences assigned to chloroplasts, mitochondria, or non-target taxa were removed.

In this study, a total of 25,558 bacterial ASVs and 5,808 fungal ASVs were obtained, with minimum sequencing depths of 28,467 and 41,837 reads per sample, respectively. The ASV tables were rarefied to these minimum depths to normalize sequencing depth across samples for downstream analyses. To minimize potential artifacts and spurious sequences generated during PCR amplification and sequencing, ASVs with a total read count of less than 2 across all samples were removed, resulting in 5,339 bacterial ASVs and 2,298 fungal ASVs retained for microbial community analyses (Table S2). Microbial α-diversity and β-diversity were calculated using the vegan package in R. To reduce the influence of false-positive correlations, CLR-transformed microbial ASV data were used to calculate Spearman correlations between ASVs. Only significant correlations with $|r| \geq 0.8$ and a Benjamini–Hochberg false discovery rate (FDR)–adjusted $P < 0.01$ were retained for network construction. Network topology was analyzed in R using the igraph package, and visualization was performed in Gephi (v0.9).

Root exudate metabolite binning and microbial community assembly mechanisms

To quantify the molecular structure similarity of RE metabolites, this study characterized metabolites across three dimensions: molecular composition, encompassing carbon and total atom counts along with elemental ratios (O/C, H/C, N/C); molecular structure, including double bond equivalents (DBE), modified aromaticity index (AI_mod), Kendrick mass defect (KMD_CH2), and 166-bit MACCS structural fingerprints; and biochemical properties, including nominal oxidation state of carbon (NOSC) and Gibbs free energy of oxidation (ΔG_ox). Detailed definitions, ecological significance, and calculation methods for these metrics are provided in Table S1. The analysis workflow involved converting metabolite SMILES strings into binary MACCS fingerprints using the rcdk package in R, then combining these fingerprints with standardized continuous variables. A Gower distance matrix was calculated via the FD package to accommodate the mixed-type data, and a molecular structure similarity tree was constructed using the Neighbor-Joining (NJ) method with the ape package. The resulting Newick format tree was then used within the iCAMP analytical framework to bin metabolites based on phylogenetic binning (Ning et al., 2020).

To quantify the relative contributions of deterministic and stochastic processes to the assembly of soil microbial communities, we employed the iCAMP framework (Ning et al., 2020). Based on the 16S rRNA gene phylogenetic tree for bacterial communities and the ITS-based phylogenetic tree for fungal communities, microbial taxa were partitioned into phylogenetic bins separately. Subsequently, βNTI (null model-based phylogenetic metric) and RC_{bray} (taxonomic metric) were calculated at the bin level. Community turnover was categorized into five assembly processes, including Heterogeneous Selection (βNTI < − 1.96), Homogeneous Selection (βNTI > 1.96), Dispersal Limitation (|βNTI| ≤ 1.96 and RC_{bray} > 0.95), Homogenizing Dispersal (|βNTI| ≤ 1.96 and RC_{bray} < − 0.95), and Drift and Others (|βNTI| ≤ 1.96 and $|RC_{bray}|$ ≤ 0.95). The relative importance of each process was then calculated across all bins to obtain assembly profiles at both the whole-community and individual-sample levels. Finally, the results were visualized using the ggplot2 package in R.

Statistical analysis

To investigate the effects of grazing on RE metabolites, microbial communities, and the consequent soil physicochemical factors, a multi-level analytical framework was employed. First, two Mantel tests were conducted using the vegan package to evaluate the correlations between metabolite bins and soil factors with microbial community assembly, and to preliminarily identify key soil factors significantly associated with both the metabolites and microbial community structure. Subsequently, co-inertia analysis (CIA, ade4 package) was applied to quantify the co-variation between the RE metabolites and microbial communities. Next, variance partitioning analysis (VPA, vegan package) was used to assess the independent and shared contributions of the RE metabolites and soil physicochemical properties to variations in microbial community composition, abundance, and phylogenetic structure. Distance-based redundancy analysis (db-RDA, vegan package) was then employed to identify the metabolite bins and soil factors that predominantly influence microbial community structure. Association networks between metabolites within specific bins and microbial communities were constructed using the igraph package (with network construction parameters consistent with those used for co-occurrence networks). Subsequently, negative binomial regression models were fitted using metabolite node degree as the response variable and ΔG_ox and molecular structural complexity index (derived from PubChem, https://www.ncbi.nlm.nih.gov/) as explanatory variables, to assess whether the functional influence of RE is constrained by thermodynamic properties and molecular structural complexity. Finally, piecewise structural equation modeling (pSEM, piecewiseSEM package) was performed to elucidate the potential pathways through which STG and LTG influence microbial communities via alterations in soil properties and RE.

All analytical details are provided in the figure legends, and data were transformed or standardized when necessary (e.g., Hellinger transformation or Z-score standardization). All analyses were performed in R version 4.4.3.

Results

Effects of grazing on the physicochemical properties of rhizosphere soil

Grazing has varying degrees of impact on the physicochemical properties of the rhizosphere soil. Specifically, STG increased rhizosphere soil nutrient levels, resulting in significantly higher TC, TN, TP, and NO_3^- compared with NG ($P < 0.05$, Table S3). However, as grazing duration increased, these nutrient levels declined and returned to levels comparable to those observed under NG. In addition, moderate grazing (MG, including SMG and LMG) significantly reduced AP relative to light grazing (LG, including SLG and LLG; $P < 0.05$, Table S3). MBN showed a variation pattern similar to that of TN across grazing treatments ($P < 0.05$; Table S3), whereas MBC showed no significant change. Grazing had limited effects on rhizosphere soil enzyme activities, with LG significantly reducing DHA activity compared with NG ($P < 0.05$, Table S4). These results suggest that STG enhanced rhizosphere nutrient availability, whereas LTG gradually diminished this effect.

Effects of grazing on root exudate metabolomics and rhizosphere microbial communities

We performed LC–MS/MS-based metabolomic profiling of *S. grandis* to assess the impacts of grazing intensity and duration. This analysis detected over 2,000 mass peaks, of which 976 plant-derived metabolites were successfully annotated (Fig. S1). Terpenoids, lipids, and amino acids and derivatives were the dominant components of the RE metabolites, collectively accounting for 62% of all annotated metabolites (Fig. S1). PLS-DA revealed distinct clustering of RE metabolites across grazing treatments (PERMANOVA, $R^2 = 0.34$, $F = 3.44$, $P < 0.001$; Fig. 1A). Grazing also caused clear changes in the abundance of RE metabolites. Compared with NG, SLG and SMG altered the abundance of 65 and 83 metabolites, respectively ($P < 0.05$; Fig. 1B). Most of these responsive metabolites increased significantly, with only one decreasing significantly in both SLG and SMG compared with NG; about 33% of the differential metabolites were shared between SLG and SMG ($P < 0.05$; Fig. 1B, Table S5). At the same grazing duration, MG resulted in more differential metabolites than LG ($P < 0.05$; Fig. 1B).

Overall, grazing had limited impact on the alpha diversity of rhizosphere microbial communities. Compared with NG, bacterial richness tended to be higher under STG (Fig. 1C). Specifically, light grazing sustained this increasing trend, resulting in significantly higher richness in LLG than in NG ($P < 0.05$; Fig. 1C). In contrast, under moderate grazing, richness declined with grazing duration, with LMG returning to levels comparable to NG (Fig. 1C). Regarding the fungal community, however, no significant changes were observed in alpha diversity across grazing treatments ($P > 0.05$; Fig. 1D). PCoA based on Bray–Curtis distances revealed significant shifts in the structure of both bacterial and fungal communities across grazing treatments (Fig. 1E and F). PERMANOVA further confirmed that grazing intensity and duration significantly altered rhizosphere microbial community composition (Bacterial: $R^2 = 0.34$, $F = 3.15$, $P < 0.001$; Fungal: $R^2 = 0.34$, $F = 3.20$, $P < 0.001$; Fig. 1E and F). To elucidate the ecological processes underlying rhizosphere microbial assembly, we applied the iCAMP framework to quantify the relative contributions of deterministic and stochastic processes. The results revealed that ecological

drift was the primary driver of rhizosphere microbial assembly, accounting for approximately 50% of the variation across all treatments (Fig. 2B and C). Beyond ecological drift, bacterial assembly was predominantly influenced by homogenizing selection (26–31%; Fig. 2B), whereas dispersal limitation (23–34%) was the key driver of fungal communities (Fig. 2C). For the bacterial community, deterministic processes remained stable across all grazing treatments (Fig. 2E). However, STG significantly increased dispersal limitation while decreasing homogenizing dispersal ($P < 0.05$; Fig. 2E). This increase in dispersal limitation was sustained under light grazing as grazing duration increased (LLG > NG; $P < 0.05$), but returned to the NG level under LMG (Fig. 2E). Unlike the bacterial community, although STG increased the contribution of dispersal limitation relative to NG, this effect diminished under LLG, returning to the NG level. In contrast, the elevated dispersal limitation was sustained under LMG (Fig. 2F). Collectively, these results indicate that grazing influenced rhizosphere microbial community structure and assembly processes, with bacterial and fungal communities exhibiting distinct responses to grazing intensity and duration.

To reduce high-dimensional redundancy and capture shared biological signals, we grouped metabolites into bins based on molecular structure similarity as representative variables, under the assumption that metabolites within each bin have analogous structures and potentially similar biological functions. These bins, together with soil physicochemical properties, were analyzed using Mantel tests to examine their associations with dispersal limitation (Kruskal-Wallis test: Bacteria $P = 0.01$, Fungi $P = 0.00$) and homogenizing dispersal (Kruskal-Wallis test: Bacteria $P = 0.00$, Fungi $P = 0.19$) (Fig. 2E and F). This approach allows identification of key RE metabolites and edaphic factors associated with stochastic shifts in rhizosphere community assembly under grazing pressure. Results indicate that dispersal limitation of rhizosphere communities was significantly associated with metabolite bins and soil physicochemical properties. A group of bins (e.g., Bins 2, 3, and 21) and soil properties such as MC and TC showed significant correlations with the dispersal limitation of both bacterial and fungal communities. In contrast, TP and NO_3^- were specifically correlated with fungal dispersal limitation ($P < 0.05$; Fig. 2G). No significant correlations were observed between any bins or soil properties and the homogenizing dispersal of either community (Fig. S2).

Root exudate metabolites act as primary drivers of changes in rhizosphere microbial community structure

To explore the relationships between RE metabolites and microbial communities, as well as their potential associated factors, we assessed the coordinated changes of RE metabolites, soil physicochemical properties, and microbial community structures, including both taxonomic and phylogenetic composition (Fig. 3). Mantel tests were then used to preliminarily identify soil physicochemical properties associated with RE metabolites and microbial communities. The results showed that bacterial and fungal communities shared a similar set of soil factors, both exhibiting significant correlations with various soil physicochemical properties (e.g., MC, TC, and TN; $P < 0.05$; Fig. S3). Notably, in addition to these factors, the RE metabolites were also significantly correlated with UE, DHA, and CL ($P < 0.05$; Fig. S3). CIA revealed significant co-variation between RE metabolites and

rhizosphere microbial community structures (Fig. 3A and B). The coupling between metabolites and microbial communities was stronger for fungi (RV = 0.59, $P < 0.01$) than for bacteria (RV = 0.49, $P < 0.01$) (Fig. 3A and B). Furthermore, VPA based on Bray–Curtis distances of microbial communities further indicated that RE metabolites contributed more independently to the variation in community composition and abundance than soil factors (Fig. 3C and D). Specifically, RE metabolites independently explained 28% and 26% of the variation in bacterial and fungal communities, respectively, both exceeding the explanatory power of soil factors (17% and 16%, respectively; $P < 0.05$; Fig. 3C and D). Procrustes analysis based on molecular structure similarity distances and microbial phylogenetic distances revealed that RE metabolites were significantly correlated only with the fungal community ($M^2 = 0.81$, $P < 0.01$; Fig. 3F). Consistently, VPA based on phylogenetic distances showed that for the bacterial community, only the independent effect of soil factors was statistically significant ($R^2 = 0.14$, $P < 0.05$; Fig. 3G). In explaining the phylogenetic variation of the fungal community, RE metabolites independently accounted for 19% of the variance ($P < 0.05$), while their joint effect with soil factors explained an additional 14% (Fig. 3H). We further employed RDA to identify metabolite bins and soil factors significantly associated with microbial community composition and abundance. The results indicated that Bin 1, Bin 2, Bin 5, Bin 16, and MC were significantly correlated with both bacterial and fungal communities ($P < 0.05$; Fig. 3I, 3J, Table S6, and S7). In addition, the bacterial community was also significantly associated with AP ($P < 0.05$; Fig. 3I and Table S6), whereas the fungal community showed additional significant correlations with TN, pH, Bin 3, and Bin 31 ($P < 0.05$; Fig. 3J and Table S7). Notably, Bins 2 and 16, as well as Bins 2 and 3, were identified as consensus variables significantly influencing dispersal limitation and community structure (composition and abundance) of bacterial and fungal communities, respectively ($P < 0.05$; Fig. 2G, 3I, and 3J). Collectively, these results indicate that RE metabolites were more strongly associated with rhizosphere microbial community variation than soil factors, with a particularly strong linkage to fungal communities.

Heatmap revealed that metabolites within Bins 3 and 16 exhibited a consistent unimodal response to grazing, with relative abundances increasing under STG before returning to NG levels under LTG (Fig. 3K). In contrast, Bin 2 exhibited a U shaped pattern, with relative abundance initially decreasing and then increasing (Fig. 3K). In addition, metabolites in Bin 2 and Bin 3 were predominantly classified as alkaloids and derivatives and indoles and derivatives, respectively, whereas most components in Bin 16 were identified as lipids (Figs. 3K and S1). To further investigate functional shifts in RE, KEGG pathway enrichment analysis was conducted for the key bins (Bins 2, 3, and 16). The results indicated that grazing significantly altered the metabolite profile relative to NG, with SMG exhibiting the most extensive metabolic response. Specifically, SMG showed the highest number of significantly enriched pathways (nine pathways, $P < 0.05$), including Tryptophan metabolism, alpha-Linolenic acid metabolism, and Aminoacyl-tRNA biosynthesis (Fig. S5). The Sankey diagram further illustrated the specific metabolites contributing to these enriched pathways. L-tryptophan, indole-3-acetic acid (IAA), and 3-indoleacetonitrile were the primary contributors to the enrichment of Tryptophan metabolism across grazing treatments. Notably, certain pathways, such as Nucleotide metabolism and Biosynthesis of amino acids, were uniquely or more strongly enriched in SMG ($P < 0.05$; Fig. S5). Collectively, these results indicate that key

metabolites exhibited distinct grazing response patterns and that SMG induced the most pronounced functional shifts in RE metabolites.

Linking metabolites and microbes through networks: metabolite characteristics and microbial topological status

We constructed microbial co-occurrence networks and metabolite–microbial interaction networks under different grazing treatments. The topological properties of rhizosphere bacterial and fungal co-occurrence networks changed divergently under STG. In bacterial networks, STG increased the number of edges relative to NG (5,697), with SLG reaching 13,397 edges. The proportion of positive correlations in bacterial networks increased from 54% in NG to 57% in SLG and 60% in SMG (Fig. 4A and Table S8). Additionally, both the average path length and the modularity of the bacterial networks followed a pattern of initially decreasing and subsequently increasing across the grazing intensity gradient (Fig. 4A and Table S8). In contrast, the fungal networks under STG exhibited a smaller scale than those in NG. Specifically, the number of edges decreased from 1,398 in NG to 1,084 in SLG and 1,114 in SMG. Correspondingly, the average degree declined from 10.47 (NG) to 8.37 (SLG) and 8.28 (SMG) (Fig. 4B and Table S9). Other topological properties of the fungal networks remained relatively stable across all treatments (Fig. 4B and Table S9). Under LTG, the structural characteristics of rhizosphere bacterial and fungal co-occurrence networks showed similar response patterns. Specifically, LLG exhibited the largest network sizes among all grazing treatments, characterized by the highest number of edges (19,650) and average degree (55.78) in the bacterial network, as well as the highest values in the fungal network (1,625 edges and an average degree of 14.98; Fig. 4A, 4B, Tables S8 and S9). Conversely, LMG resulted in the smallest networks across treatments; bacterial edge count and average degree decreased to 5,083 and 14.71, respectively, while the fungal network also reached its lowest connectivity (1,348 edges and an average degree of 8.36), despite being supported by the highest number of nodes (Fig. 4A, 4B, Tables S8 and S9).

Interaction networks were constructed using key metabolite bins (Bins 2, 3, and 16) to identify microbial taxa potentially associated with RE metabolites. The relative degree metric was applied to enable direct comparisons across treatments. The results indicated that the relative degree of these microbes potentially associated with metabolites in the interaction networks was significantly lower under STG than in other treatments (bacteria: NG, LLG, and LMG; fungi: NG and LLG; $P < 0.05$; Fig. 4C and 4D). Furthermore, simulated extinction of these metabolite associated taxa was performed to evaluate microbial community stability using natural connectivity. The results indicated that bacterial community stability was significantly correlated with metabolites in RE in three grazing treatments (SMG: $R^2 = 0.46$; LLG: $R^2 = 0.95$; LMG: $R^2 = 0.21$; all $P < 0.001$; Fig. 4E). While fungal community stability showed significant correlations with metabolites in RE across all grazing treatments, the weakest associations were observed under STG (SLG: $R^2 = 0.38$; SMG: $R^2 = 0.18$; all $P < 0.001$; Fig. 4F). Negative binomial regression models were employed to assess the functional efficiency of metabolites by examining the associations between their node degree in the interaction networks and their corresponding ΔG_ox and molecular structure index. The results indicated that the ΔG_ox of metabolites was significantly

correlated with the degree of Bin 2 only in the bacterial interaction network under LMG (R^2 = 0.16, P < 0.05; Fig. S4C). In contrast, the molecular structural complexity index of metabolites exhibited widespread significant correlations with their degrees in both bacterial and fungal interaction networks. Specifically, in NG, the molecular structural complexity index of Bin 2 was significantly correlated with its degree in both bacterial (R^2 = 0.13, P < 0.05) and fungal (R^2 = 0.29, P < 0.001) interaction networks (Fig. S4E and S4F). Furthermore, under LMG, the molecular structural complexity index of Bin 16 and Bin 2 showed significant correlations with their degrees in the bacterial (R^2 = 0.16, P < 0.05) and fungal (R^2 = 0.22, P < 0.01) interaction networks, respectively (Fig. S4E and S4F).

The primary microbial responders to root exudates shifted with grazing duration

Finally, piecewise structural equation modeling (pSEM) was performed to decipher the causal pathways among grazing intensity, RE metabolites, rhizosphere soil physicochemical properties, community assembly processes, and microbial community structure. For the STG model (Fisher's C = 7.317, df = 8, P = 0.503; Fig. 5A), results indicate that STG altered the expression of RE metabolites (R = 0.60, P < 0.01), which in turn influenced the structure of rhizosphere bacterial community (R = 0.60, P < 0.05; Fig. 5A). Moreover, STG (R = 0.31, P < 0.05) and RE metabolites (R = 0.63, P < 0.001) have influenced the physicochemical properties of the rhizosphere soil (Fig. 5A). For the LTG model (Fisher's C = 7.723, df = 8, P = 0.461; Fig. 5B), no significant effects of grazing or RE on bacterial community structure were observed. Instead, the direct action of grazing (R = 0.40, P < 0.05) and the mediated effects of RE metabolites (R = 0.79, P < 0.001; R = 0.58, P < 0.05) significantly altered fungal community structure (Fig. 5B). Collectively, these results indicate that grazing effects on rhizosphere microbial communities are mediated by RE, with bacteria responding predominantly under STG and fungi under LTG.

Discussion

Understanding RE metabolites and its influence on rhizosphere microbial communities enhances our knowledge of grassland plant-soil microbe crosstalk and supports the sustainable health of grassland ecosystems(Sasse et al., 2018; Yang et al., 2026). However, the difficulty in obtaining RE in natural environments and the flexibility of metabolite-mediated strategies under varying grazing conditions pose challenges to understanding this relationship.

In this study, we collected in *situ* RE of *S. grandis*, the dominant species in the temperate grasslands of Inner Mongolia under varying grazing intensities. Adapting the ecological framework for community assembly, we applied the β-nearest taxon index (βNTI) and Raup–Crick (RC) metrics to quantify the processes governing the exudate metabolites (Ning et al., 2020). However, due to the fundamental differences between the continuous nature of metabolomics data and the sparsity of microbial datasets, determination of ecological processes should be made cautiously. Nevertheless, integrating SMILES of metabolites with molecular elemental composition (e.g., C, N, and H atom counts), in a manner analogous to microbial phylogeny, enables the quantification of molecule structural similarity at

substantially higher resolution than atomic counts alone (Weininger, 1988). Thus, treating metabolite bins as variables remains a robust strategy for elucidating their interactions with rhizosphere communities.

Potential rhizosphere priming and resource pulses under short-term grazing

The addition of fresh C substrates to soil can accelerate or retard the decomposition of soil organic matter (SOM), a phenomenon termed the priming effect (PE), or rhizosphere priming effect (RPE) when driven by root activity (Favaro et al., 2025). In grassland ecosystems, grazing is a primary driver of this process. The effects of grazing arise from multiple factors, including accelerated nutrient inputs from trampling and excreta deposition, as well as grazing induced plant stress that can enhance root turnover and stimulate the secretion of RE (Xun et al., 2018). These combined inputs of labile C may generate a resource pulse that promotes potential RPE, thereby enhancing microbial activity and facilitating the transient accumulation of available nutrients (Favaro et al., 2025; He et al., 2025). In this study, we also observed an enrichment of rhizosphere soil nutrients under STG (Table S3). Notably, given that RE represent a primary source of DOC, this finding is supported by our metabolites data, which revealed a significant upregulation of numerous metabolites under STG (Table S5, Fig. 1B). As typical r-strategists, copiotrophic bacteria generally exhibit high metabolic activity and growth rates (Zhu and Dai, 2024). Consequently, they may derive considerable benefit from such environments, potentially proliferating rapidly within a short timeframe, which could contribute to higher taxonomic richness and an expanded network size (Fig. 1C, 4A and Table S8). Overall, the coupling of belowground resource pulses with bacterial life-history strategies provides a plausible framework for understanding these initial structural shifts in the rhizosphere community.

Ecological filtering and niche differentiation under long-term grazing intensity gradients

Unlike the potential PE driven by resource pulses observed in STG, the response of rhizosphere microbial communities under LTG exhibits marked differences. Our results demonstrate found that LLG helps maintain higher bacterial diversity, whilst the co-occurrence networks of bacteria and fungi also become more complex (Fig. 1C, Table S8 and S9). This change in community structure may be primarily attributed to the synergistic interactions between aboveground and belowground ecological processes under light disturbance (Ju et al., 2026). Livestock grazing reduces litter accumulation, potentially improving soil aeration (Li et al., 2024); additionally, the continuous input of excreta provides stable and readily available N sources, thereby accelerating the system's nutrient cycling (Zhou et al., 2017). Another noteworthy factor is that as grazing duration progresses, plants may undergo a physiological transition where RE patterns shift from acute stress-induced surges to the re-establishment of stable rhizosphere signaling (Ma et al., 2025). This ecological inference is further supported by relative degree comparisons and simulated species extinction analyses. Most microbial taxa potentially associated with RE metabolites occupied key positions in their respective co-occurrence networks (Fig. 4C and D),

resembling patterns observed in the NG. Moreover, these taxa were shown to be critical for supporting community stability (Fig. 4E and 4F).

However, when grazing intensity further increases and is maintained over the long term, the aboveground–belowground coordination sustained by light disturbance may be disrupted, and the composition of the rhizosphere microbial community shifts toward being shaped by ecological filtering alongside mutualistic and competitive interactions under chronic stress (Du et al., 2025; Huang et al., 2026). The massive loss and continuous exposure of surface vegetation induced by LMG likely exacerbates soil microclimate fluctuations (e.g., moisture) and physical compaction, thereby restricting aboveground-to-belowground C inputs (Liu et al., 2025; Zhang et al., 2026).

Although elevated livestock density increases excreta deposition, the chronic deficit of plant-derived C may constrain the effective microbial assimilation of excreta-derived N (Wang et al., 2023). Concurrently, soil compaction could reduce N infiltration rates; together, these processes are likely to drive a continuous loss of ecosystem resources (Li et al., 2024). Our results further corroborate this resource-limited state. Multiple rhizosphere soil physicochemical indicators under LMG decreased to their lowest levels across all treatments (e.g., TN, TC, TP, Table S3). Concurrently, the α-diversity of the bacterial community decreased, and the scale of the co-occurrence network contracted substantially (Fig. 1C and Table S8). Notably, increased network modularity and a higher proportion of negative edges suggest that, rather than a uniform decline under chronic heavy stress (Table S8), the bacterial community shifted toward greater functional compartmentalization and intensified resource competition (Liu et al., 2025). In contrast, the diversity of the fungal community remained relatively stable, potentially reflecting its stronger stress tolerance (Fig. 1D). The response of the fungal co-occurrence network to LMG was similar to that of bacteria; however, a key difference was that a greater number of taxa were involved in the network construction (Table S9). This expanded participation may be related to the specific recruitment of fungi by plant RE, which will be discussed further below (Sasse et al., 2018).

Root exudates play a non-negligible driving role on rhizosphere microbial community composition under grazing

Our findings show that under grazing stress, the RE metabolites of *S. grandis* not only couple with the rhizosphere microbial community but also acts as a key driver of microbial community structural shifts (Figs. 3A–D). It is plausible that *S. grandis* does not merely endure herbivory passively; rather, it likely actively drives rhizosphere microbial changes by reallocating belowground carbon and releasing specific signaling metabolites (Sasse et al., 2018). This potentially establishes positive plant-microbe feedbacks that aid in compensatory growth and post-grazing recovery (Li et al., 2025). Although RE exert a pronounced driving force on rhizosphere microbial community structure, the “biochemistry dialogue” between *S. grandis* and different microbial taxa is notably asymmetric, with phylogenetic coupling observed only with the fungal community (Fig. 3E-H). The profound evolutionary coupling between plants and fungi reflects their ancient symbiotic history, particularly with arbuscular mycorrhizal (AM)

fungi, as evidenced by conserved signaling amplifiers such as the kinases MtLICK1/2 (Wang et al., 2025a). Moreover, robust extracellular enzyme systems enable fungi to efficiently degrade complex organic matter (e.g., lignin and cellulose), while extensive hyphal networks expand their spatial reach for resource acquisition and confer strong environmental resilience (Martin and Tan, 2025). Consequently, fungal α-diversity remained stable even under LMG (Fig. 1D). Under prolonged environmental stress, plants may therefore preferentially deploy conserved metabolic signals to directionally recruit specific fungal lineages (Fig. 5B), forging stable mutualisms for long-term stress tolerance (Vernié et al., 2025).

Recruiting beneficial microbes via RE is a core plant adaptation to biotic and abiotic stresses (Sasse et al., 2018). The key metabolic bin (Bin 16) driving rhizosphere bacterial community structure in our study predominantly comprised lipid metabolites, whose relative abundance increased under STG (Fig. 3K). Compared to amino acids and other secondary metabolites, lipids generally possess a higher thermodynamic energy density (Zhang et al., 2025). Thus, the targeted allocation of these high-energy exudates belowground during early grazing likely provides an exceptionally efficient carbon and energy substrate, fueling the rapid proliferation of fast-growing bacteria and driving structural shifts within the community (Fig. 1C and 5A). Furthermore, KEGG enrichment revealed that grazing altered the functional pathways of *S. grandis* RE, triggering intense cross-kingdom communication during the early grazing response (Fig. S5). Tryptophan, a precursor for key signaling molecules like auxin (IAA) and melatonin, is typically enriched during early stress responses (Wang et al., 2025b). Aligning with this strategy, "Tryptophan metabolism" exhibited higher enrichment under STG than LTG (Fig. S5). Previous studies have demonstrated that soil bacteria can utilize plant-derived tryptophan to synthesize host-promoting IAA (Patel et al., 2025). In parallel, "alpha-Linolenic acid metabolism" was specifically enriched under SMG (Fig. S5); its core product, jasmonic acid (identified here as the isomer (-)-jasmonic acid), is a key signaling molecule known to directionally recruit beneficial taxa such as *Pseudomonas* (Yang et al., 2025). Collectively, these results suggest that *S. grandis* may respond to early grazing stress by releasing energy-rich lipid substrates that stimulate bacterial proliferation, while simultaneously secreting specific signaling molecules (tryptophan and (-)-jasmonic acid) to regulate microbial communities. However, prolonged grazing shifted this biochemistry strategy; alongside tryptophan metabolism, only "Benzoxazinoid biosynthesis" and "Caffeine metabolism" remained significantly enriched (Fig. S5). Benzoxazinoids are typical defensive secondary metabolites in Poaceae grasses (Kudjordjie et al., 2019). In related species (e.g., maize and wheat), these metabolites exert much stronger regulatory effects on fungal than bacterial communities, positively correlating with specific fungal taxa like *Stemphylium*, *Vishniacozyma*, and *Didymella* (Wilkes et al., 1999; Martyniuk et al., 2006). Therefore, under prolonged herbivory, *S. grandis* likely sustains the secretion of these defensive metabolites to achieve persistent, directional regulation of the rhizosphere fungal community as a key adaptive strategy to continuous grazing stress (Fig. 5B).

Trade-offs in the characteristics of metabolites in root exudates under grazing

Prolonged heavy grazing severely limits plant carbon assimilation capacity (Sanaei et al., 2023), potentially forcing a trade-off between the energy costs and signaling efficiency of RE-mediated cross-kingdom communication (Wang and Kuzyakov, 2024). Based on a preliminary analysis of metabolite ΔG_ox and molecular structural complexity index, this study offers an initial biochemical and thermodynamic perspective on the potential rules governing this trade-off. These findings provide a reference and inspiration for future research aimed at unraveling the mechanisms of plant-microbe communication under extreme stress.

We found that only under LMG were the topological positions of Bin 2 metabolites within metabolite–bacteria interaction networks significantly constrained by thermodynamic properties (Fig. S4C). A more negative ΔG_ox corresponds to a higher degradation energy yield (Wu et al., 2025), and the constituent alkaloids and amino acids, as nitrogenous metabolites (Fig. 3K), also serve as potential nitrogen sources (Coskun et al., 2017). This suggests that *S. grandis* may upregulate these metabolites under the dual stress of soil nutrient limitation and the aboveground carbon deficit induced by LMG, with their topological positions in bacterial interactions exhibiting a thermodynamic hierarchical differentiation (i.e., higher energy metabolites occupy higher topological positions, and vice versa) (Fig. S4C). By contrast, the relatively abundant labile nutrient inputs under NG and short-term grazing mitigated this substrate constraint, decoupling metabolite thermodynamic properties from the network topology (Fig. S4C). Unlike bacteria, which are constrained by substrate energetics, fungal communities exhibited a distinct niche advantage in overcoming thermodynamic barriers (Fig. S4D). This is likely attributable to their extensive hyphal networks and robust extracellular enzyme systems, which endow them with superior substrate versatility and environmental buffering capacity in acquiring and degrading complex organic matter (Martin and Tan, 2025).

In closed and relatively stable systems (NG) and resource constrained systems (LMG) (Table. S1), *S. grandis* likely regulates microbial communities through RE based on the specific structures of metabolites rather than energy gradients (Sasse et al., 2018). These significant associations between metabolite molecular structural complexity index and network topological positions suggest that *S. grandi***s** can efficiently regulate rhizosphere microbial communities by expending less fixed carbon (Fig. S4E and S4F). However, compared with NG, STG disturbance altered this relatively stable chemical communication pattern. The plant stress response induced by STG likely increased carbon allocation belowground, facilitating rapid microbial utilization of low complexity and easily degradable metabolites (Chen et al., 2021). This manifests as a negative correlation between metabolite complexity and network topological positions (Fig. S4E and S4F). Concurrently, plants may activate biochemical signaling pathways associated with defense, upregulating the secretion of indole metabolites as stress signals to regulate rhizosphere microbial communities and mitigate grazing stress (Kazarina et al., 2025). The positive correlation between the complexity of Bin 3 metabolites and network topological positions under SMG provides support for this regulatory process (Fig. S4F). Admittedly, the modest explanatory power (R^2) of these associations may warrant cautious interpretation. This pattern may partly reflect the stringent analytical framework, in which strict microbial filtering and a focus on selected metabolite bins capture only a reduced fraction of the overall biochemical dialogue, potentially excluding rare taxa and

alternative metabolic pathways and thereby constraining the observed R^2. In short, from NG to LMG, the strategy of *S. grandis* to regulate microbial communities via RE likely dynamically transitioned from specific homeostatic regulation, through a generalized carbon pulse driven by disturbance, to the formation of a new steady state structure dictated by carbon resource utilization tradeoffs.

Conclusion

This study demonstrates that root exudates of *Stipa grandis* play a dominant role in shaping the structure of rhizosphere microbial communities under grazing stress, exerting a stronger influence than soil physicochemical factors. The plant adopts a temporally evolving asymmetric regulatory strategy. Under short-term grazing, the release of lipids and specific signaling molecules promotes rapid bacterial proliferation. Under long-term moderate grazing, the plant maintains the secretion of defensive metabolites and establishes stable symbiosis with fungi, supporting the persistence of the fungal community. Although this steady-state trade-off has been preliminarily revealed from biochemical and thermodynamic perspectives, single-time-point sampling cannot capture seasonal or developmental dynamics, and the thermodynamic mechanisms still require further experimental verification. Future studies integrating time-series sampling with root transcriptomics will provide deeper insights into the dynamic networks of cross-kingdom plant–microbe communication and offer theoretical support for understanding grassland ecosystem resilience and the sustainable management of degraded rangelands.

References

1. Badri DV, Vivanco JM (2009) Regulation and function of root exudates. Plant Cell Environ 32:666–681
2. Bölscher T, Cardon ZG, Arredondo MG, Grand S, Griffen G, Hestrin R, Imboden J, Jamoteau F, Lacroix EM, Castro SP, Persson P, Riley WJ, Keiluweit M (2025) Vulnerability of mineral-organic associations in the rhizosphere. Nat Commun 16
3. Che R, Wang S, Wang Y, Xu Z, Wang W, Rui Y, Wang F, Hu J, Tao J, Cui X (2019) Total and active soil fungal community profiles were significantly altered by six years of warming but not by grazing. Soil Biol Biochem 139:107611
4. Chen YJ, Neilson JW, Kushwaha P, Maier RM, Barberán A (2021) Life-history strategies of soil microbial communities in an arid ecosystem. ISME J 15:649–657
5. Coleine C, Stajich JE, Selbmann L (2022) Fungi are key players in extreme ecosystems. Trends Ecol Evol 37:517–528
6. Coskun D, Britto DT, Shi WM, Kronzucker HJ (2017) How Plant Root Exudates Shape the Nitrogen Cycle. Trends Plant Sci 22:661–673
7. Ding Y, Yao J, Li F, Hou L, Cheng J, Zhang R, Dong Y, Liu L, Sun Q (2025) Unlocking rhizosphere phosphorus: Root exudate-microbe synergy drives phosphorus activation in mixed Chinese fir

species plantation. Ind Crops Prod 237:122220

8. Du Y, Yang Y, Wu SN, Gao XX, He XQ, Dong SK (2025) Core microbes regulate plant-soil resilience by maintaining network resilience during long-term restoration of alpine grasslands. Nat Commun 16
9. Favaro A, Singh B, Warren C, Dijkstra FA (2025) Differences between priming andrhizosphere priming effects: Concepts andmechanisms. Soil Biol Biochem 205
10. Gao X, Zhang D, Peng Y, Peñuelas J, Hautier Y, Loreau M, Niu Y, Yao S, Wu Z, Li Q, Zhou L, Liu Y, Liu X, Wei B, Qin S, Song Y, Kang L, Jiang L, Wang S, Yang Y (2025) Grassland degradation alters plant and soil biodiversity–multifunctionality relationships. Nat Plants 11:2487–2497
11. Guo TT, Guo MQ, Ryo M, Rillig MC, Liu N, Zhang YJ (2025) Ungulate herbivory affects grassland soil biota β-diversity and community assembly via modifying soil properties and plant root traits. New Phytol 247:281–294
12. He FC, Dong SK, Ma CH, Hao XH, Shen H, Yang JJ, Xiao JN, Li Y, Zhang R, Shi H, Wang ZY, Zhang YH, Zuo H (2025) Grazing mediates soil nutrient stocks through changing the plant functional composition and plant biomass allocation in alpine grassland, vol 391. Agriculture Ecosystems & Environment
13. Huang JR, Cai M, Han MX, Fang BZ, Dong L, Zhang GS, Han JR, Li S, Rustamova N, Liu YH, Li WJ, Jiang HC (2026) Habitat heterogeneity drives microbial community assembly and functional specialization in extremely arid ecosystems. Appl Environ Microbiol 92
14. Ji XY, Ye C, Kang WT, Luan WJ, Liu YX, He XH, Yang M, Sun LF, Sun WS, Huang HC, Zhu YY, Zhu SS (2025) Interspecific allelopathic interaction primes direct and indirect resistance in neighboring plants within agroforestry systems. Plant Commun 6
15. Ju X, Han GD, Chen XL, Wang ZW, Li ZG, Bisseling T, Gordon I, Wu Q (2026) Grazing intensity shifts biodiversity drivers of ecosystem multifunctionality in a desert steppe. Agriculture Ecosystems & Environment 400
16. Kazarina A, Sarkar S, Adams B, Vogt B, Rodela L, Pogranichny S, Powell S, Wiechman H, Heeren L, Reese N, Thompson D, Ran QH, Hartung E, Akhunova A, Akhunov E, Johnson L, Jumpponen A, Lee STM (2025) Interaction of plant-derived metabolites and rhizobiome functions enhances drought stress tolerance. Genome Biol 26
17. Kudjordjie EN, Sapkota R, Steffensen SK, Fomsgaard IS, Nicolaisen M (2019) Maize synthesized benzoxazinoids affect the host associated microbiome. Microbiome 7.
18. Li SC, Xing TT, Sa R, Zhang YJ, Chen HY, Jin K, Shao QQ, Tang SM, Wang CJ (2024) Effects of grazing on soil respiration in global grassland ecosystems. Soil & Tillage Research 238
19. Li YL, Li FY, Shi CJ, Wang H, Wu L, Wang YD, Minggagud H (2025) Precipitation and grazing intensity jointly shape plant compensatory growth and productivity in a semi-arid steppe ecosystem. Agriculture Ecosystems & Environment 393
20. Liu YZ, Zhao XQ, Liu WT, Feng B, Lv WD, Zhang ZX, Yang XX, Dong QM (2024) Plant biomass partitioning in alpine meadows under different herbivores as influenced by soil bulk density and available nutrients. CATENA 240:108017

21. Liu Z, Shen Y, Wang GH, Li HP, Ma JL, Zhou Y, Li W, Ma HB (2025) Moderate time grazing in the warm season maintained the diversity and complexity of soil microorganisms by regulating nutrient cycling and decomposition function. Funct Ecol 39:2772–2789
22. Ma JG, Yu JF, Wang XB, Hou FJ (2025) Plant and microbial communities follow fast-to-slow strategies in response to grazing in an arid rangeland. Agriculture Ecosystems & Environment 384
23. Martin F, Tan H (2025) Saprotrophy-to-symbiosis continuum in fungi. Curr Biol 35:R469–R475
24. Martyniuk S, Stochmal A, Macías FA, Marín D, Oleszek W (2006) Effects of some benzoxazinoids on in vitro growth of and other fungi pathogenic to cereals and on stripe of winter wheat. J Agric Food Chem 54:1036–1039
25. Mendes R, Kruijt M, de Bruijn I, Dekkers E, van der Voort M, Schneider JHM, Piceno YM, DeSantis TZ, Andersen GL, Bakker PAHM, Raaijmakers JM (2011) Deciphering the Rhizosphere Microbiome for Disease-Suppressive Bacteria. Science 332:1097–1100
26. Ning D, Yuan M, Wu L, Zhang Y, Guo X, Zhou X, Yang Y, Arkin AP, Firestone MK, Zhou J (2020) A quantitative framework reveals ecological drivers of grassland microbial community assembly in response to warming. Nat Commun 11
27. Patel RR, Triplett LR, Taerum SJ, Nason SL, Wilson CO, Steven B (2025) Diverse soil protists show auxin regulated growth in partnership with auxin-producing bacteria. ISME J 19
28. Phillips RP, Erlitz Y, Bier R, Bernhardt ES (2008) New approach for capturing soluble root exudates in forest soils. Funct Ecol 22:990–999
29. Qiao Y, Wang T, Huang Q, Guo H, Zhang H, Xu Q, Shen Q, Ling N (2024) Core species impact plant health by enhancing soil microbial cooperation and network complexity during community coalescence. Soil Biol Biochem 188
30. Ren S, Terrer C, Li J, Cao Y, Yang S, Liu D (2024) Historical impacts of grazing on carbon stocks and climate mitigation opportunities. Nat Clim Change 14:380–386
31. Sanaei A, Sayer EJ, Yuan ZQ, Saiz H, Delgado-Baquerizo M, Sadeghinia M, Ashouri P, Ghafari S, Kaboli H, Kargar M, Seabloom EW, Ali A (2023) Grazing intensity alters the plant diversity-ecosystem carbon storage relationship in rangelands across topographic and climatic gradients. Funct Ecol 37:703–718
32. Sasse J, Martinoia E, Northen T (2018) Feed Your Friends: Do Plant Exudates Shape the Root Microbiome? Trends Plant Sci 23:25–41
33. Shen X, Yang F, Xiao C, Zhou Y (2020) Increased contribution of root exudates to soil carbon input during grassland degradation. Soil Biol Biochem 146
34. Sun YY, Zhang WM, Xiu LQ, Gu WQ, Wu D, Tang L, Chen WF (2025) Long-term fertilization regimes modulate dissolved organic matter molecular chemodiversity and greenhouse gas emissions in paddy soil. Biochar 7.
35. Vernié T, Rich M, Pellen T, Teyssier E, Garrigues V, Chauderon L, Medioni L, van Beveren F, Libourel C, Keller J, Girou C, Lefort C, Le Ru A, Martinez Y, Reinhardt D, Kodama K, Shimazaki S, Morel P, Kyozuka J, Mbengue M, Harrison M, Vandenbussche M, Delaux PM (2025) Conservation of symbiotic

signaling since the most recent common ancestor of land plants. Proceedings of the National Academy of Sciences of the United States of America 122

36. Wang CQ, Kuzyakov Y (2024) Mechanisms and implications of bacterial-fungal competition for soil resources. ISME J 18
37. Wang DP, Jin R, Shi XB, Guo HR, Tan XH, Zhao AC, Lian XH, Dai HL, Li SZ, Xin KX, Tian CF, Yang J, Chen WS, Macho AP, Wang ER (2025a) A kinase mediator of rhizobial symbiosis and immunity in. Nature 643
38. Wang S, Zhang X, Gong DH, Huang QQ, Kandegama WMWW, Georgiev MI, Gao YY, Liao P, Hao GF (2025b) Sophisticated crosstalk of tryptophan-derived metabolites in plant stress responses. Plant Commun 6
39. Wang XY, Li FY, Tang KY, Wang YN, Suri G, Bai Z, Baoyin T (2020) Land use alters relationships of grassland productivity with plant and arthropod diversity in Inner Mongolian grassland. Ecological Applications 30.
40. Wang Y, Niu D, Yuan X, Guo D, Fu H, Elser JJ (2023) Dominant plant species alter stoichiometric imbalances between soil microbes and their resources in an alpine grassland: Implications for soil microbial respiration. Geoderma 431:116336
41. Weininger D (1988) SMILES, a chemical language and information system. 1. Introduction to methodology and encoding rules. J Chem Inf Comput Sci 28:31–36
42. Wilkes MA, Marshall DR, Copeland L (1999) Hydroxamic acids in cereal roots inhibit the growth of take-all. Soil Biol Biochem 31:1831–1836
43. Wilson CH, Strickland MS, Hutchings JA, Bianchi TS, Flory SL (2018) Grazing enhances belowground carbon allocation, microbial biomass, and soil carbon in a subtropical grassland. Glob Change Biol 24:2997–3009
44. Wu D, Zhang MY, Hu SJ, Liu Y, Zhen F, Liu H, Sun YM (2025) Multidimensional insights into efficiency-stability trade-off in anaerobic digestion from organic overloading stress: Kinetic behavior, energy harvesting, and genome-centric metagenomics microbial self-adaptation. Water Res 284
45. Xun W, Yan R, Ren Y, Jin D, Xiong W, Zhang G, Cui Z, Xin X, Zhang R (2018) Grazing-induced microbiome alterations drive soil organic carbon turnover and productivity in meadow steppe. Microbiome 6:170
46. Yang GS, Gong JR, Zhang SP, Wang RJ, Wang T, Yu YH, Xie Q (2026) Trade-offs between root exudation and root traits induced by coexisting species under a grazing gradient can mobilize available nitrogen to promote grassland productivity. Soil & Tillage Research 260
47. Yang SD, Bezemer TM, Yuan XH, Liu XY, Wan T, Liu FH, Wen T, Shen QR, Yuan J (2025) Design of effective synbiotics against aboveground insect herbivory through characterization of host plant rhizosphere microbiota and metabolites. Mol Plant 18:1901–1919
48. Yu Y, Zhu B, Li XR, Chen X, Deng Y, Xiao CW (2026) Warming Favors Fungal Partnerships in Dominant Plants but Bacterial Alliances in Subordinate Species. Plant Cell Environ 49:2113–2115

49. Zhang JW, Sun Y, Zhang Y, Liu Y, Hou FJ (2026) Symmetric response of the temporal stability of community aboveground and belowground biomass to stocking rate and grazing season: Insights from a five-year grazing experiment in alpine meadows. Agriculture Ecosystems & Environment 398
50. Zhang Q, Wang ZQ, Gao RJ, Jiang YN (2025) Sugars, Lipids and More: New Insights Into Plant Carbon Sources During Plant-Microbe Interactions. Plant Cell Environ 48:1656–1673
51. Zhou GY, Zhou XH, He YH, Shao JJ, Hu ZH, Liu RQ, Zhou HM, Hosseinibai S (2017) Grazing intensity significantly affects belowground carbon and nitrogen cycling in grassland ecosystems: a meta-analysis. Glob Change Biol 23:1167–1179
52. Zhu ML, Dai XF (2024) Shaping of microbial phenotypes by trade-offs. Nat Commun 15

Figures

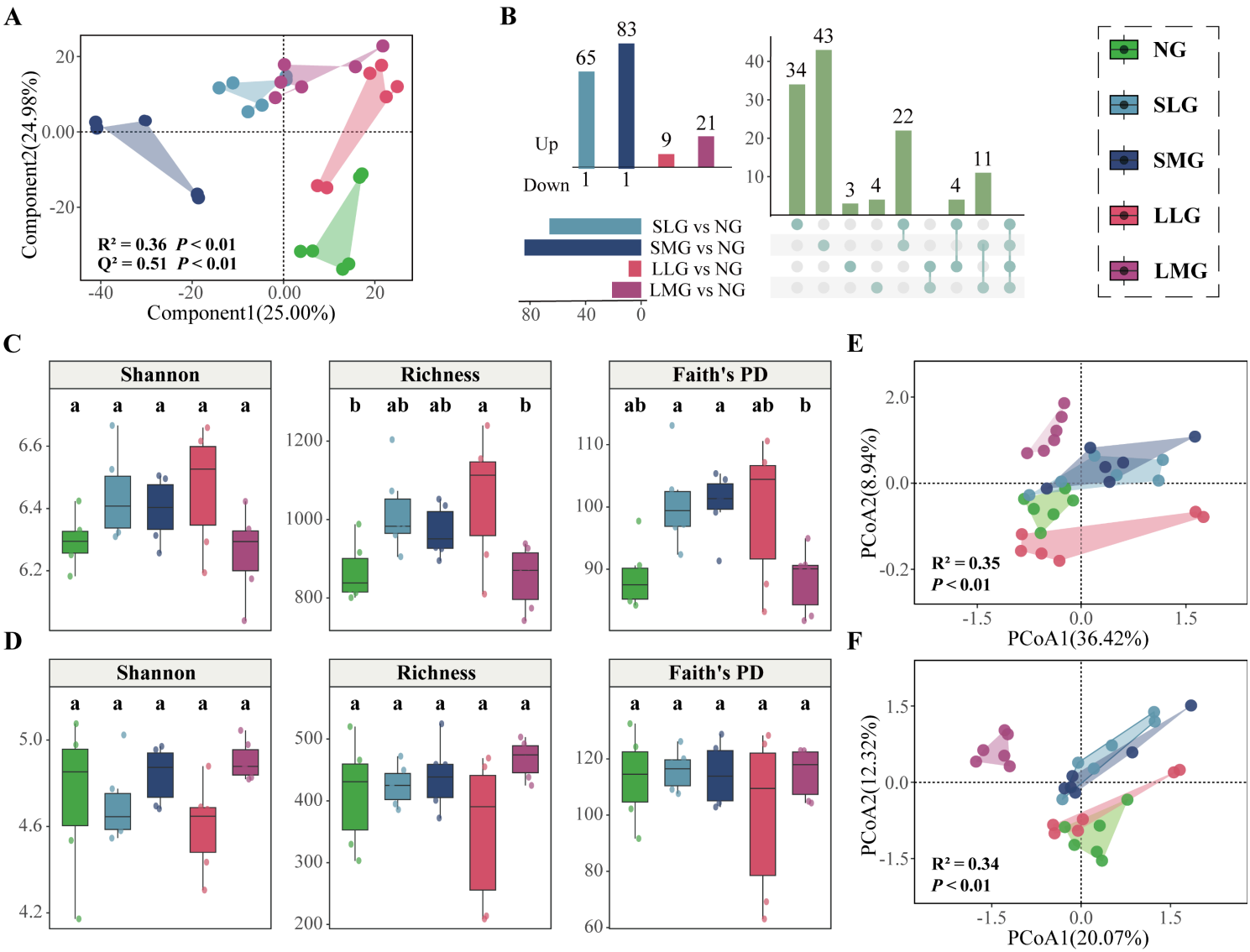

Figure 1

Fig 1. Effects of grazing on root exudates and rhizosphere microbial communities. (A) Partial Least Squares Discriminant Analysis (PLS-DA) was employed for different grazing treatments, with ADONIS based on the Euclidean distance matrix evaluating group differences in root exudate metabolites ($P < 0.05$). (B) An Upset Venn diagram of the number of different metabolites common and unique in different alignment groups. The numbers in the bar chart show the number of metabolites. Alpha diversity of rhizosphere bacterial (C) and fungal (D) communities across grazing treatments. Diversity indices were compared by one-way ANOVA followed by Tukey's HSD test when significant ($\alpha = 0.05$); different letters indicate significant differences among treatments ($P < 0.05$). Principal Coordinate Analysis (PCoA) based on Bray-Curti's distance was employed to rank bacterial (E) and fungal (F) communities in rhizosphere, with ADONIS used to assess differences between groups.

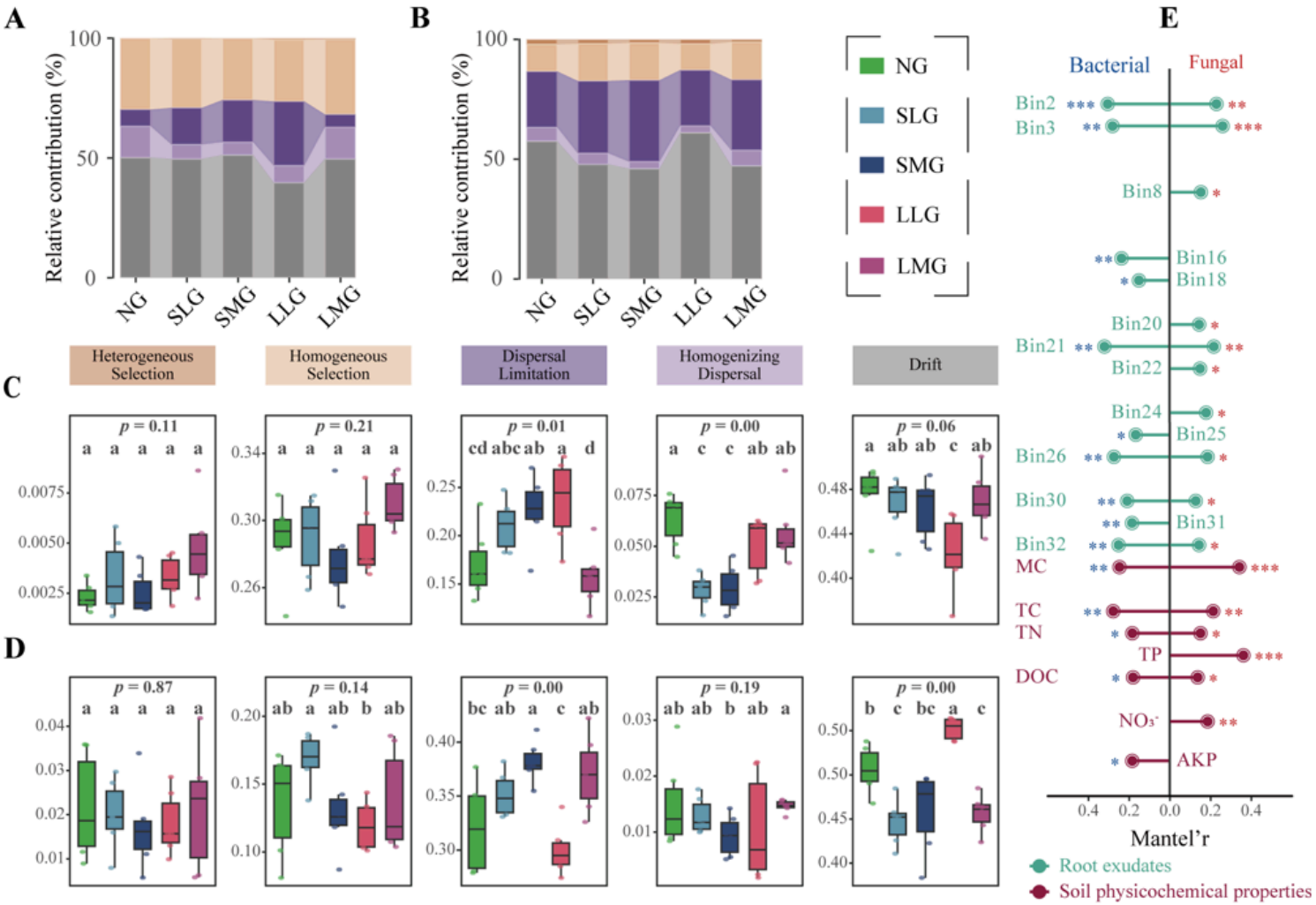

Figure 2

Fig 2. Effects of grazing on the assembly mechanisms of rhizosphere microbial communities, and their correlations. Relative contribution of bacterial (A) and fungal (B) communities across ecological processes under different grazing treatments. Changes in bacterial (C) and fungal (D) community assembly processes under different grazing treatments within the same ecological process. Differences between multiple treatments were assessed using the Kruskal-Wallis's; pairwise comparisons employed

the Wilcoxon signed-rank test. Different letters indicate significant differences among treatments ($P < 0.05$). (E) Mantel correlations (only significant variables shown) between the dispersal limitation of bacterial (left) and fungal (right) communities and both the binning of root exudate metabolites based on ICAMP analysis and rhizosphere soil physicochemical properties. *$P < 0.05$, **$P < 0.01$, **$P < 0.001$.

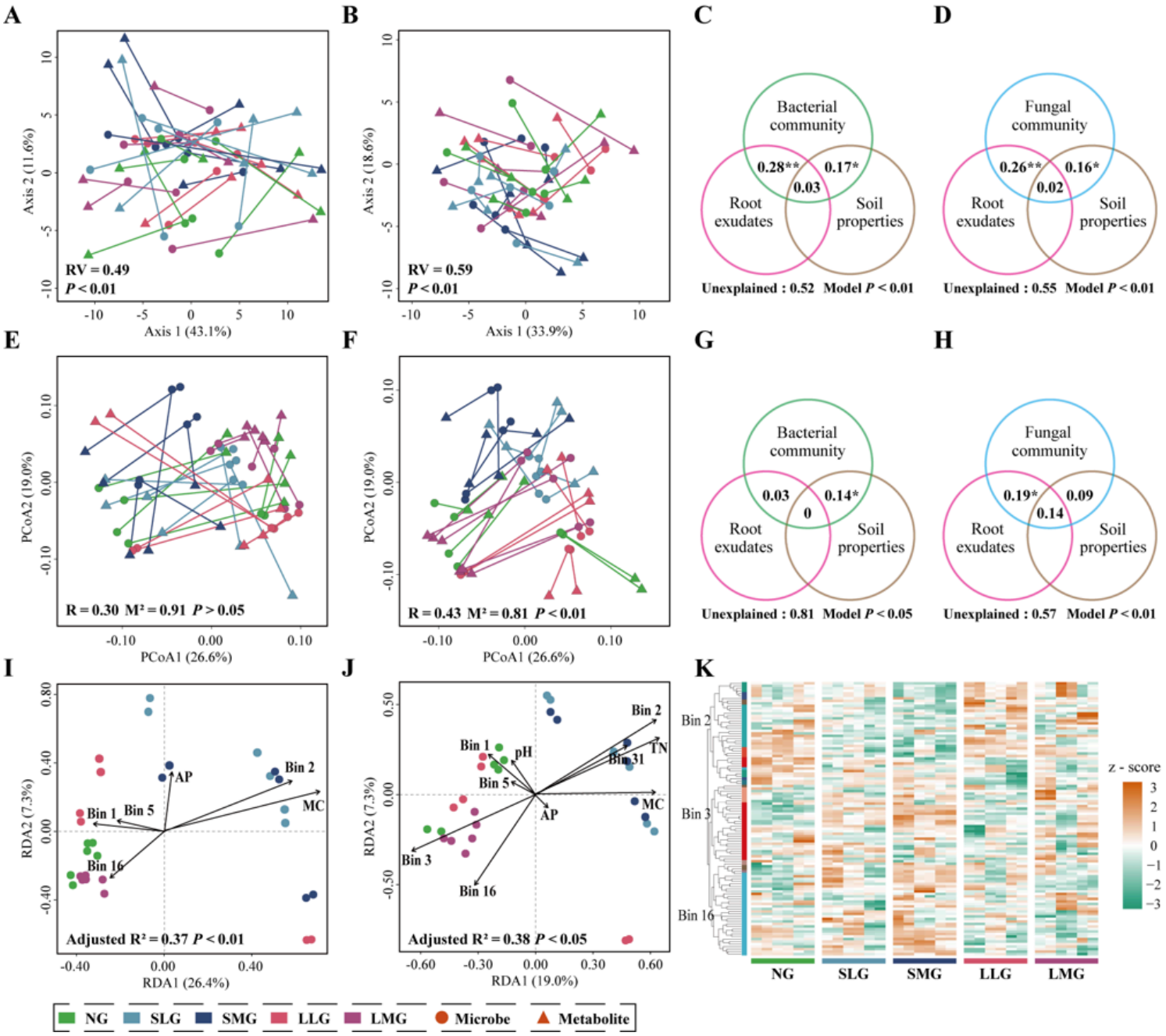

Figure 3

Fig 3. Correlation between root exudate metabolites and rhizosphere microbial communities. Co-inertia analysis (CIA) of root exudate metabolites and bacterial (A) and fungal (B) communities. RV coefficients represent the strength of the co-structure, with *P*-values derived from permutation tests (n = 999). Variation partitioning analysis (VPA) quantifies the relative contributions of root exudate metabolites and soil factors (from Mantel tests, Fig. S3: MC, TN, TC, DOC, NO_3^-, TP, AP, AKP, UE, DHA, and CL) to the

variation in bacterial (C, G) and fungal (D, H) communities. Community variation is calculated based on Bray–Curtis distance (C, D) and Weighted UniFrac distance (G, H). Metabolic predictors are represented by PCA axes capturing 90% of the variance derived from Euclidean distance (C, D) and chemical similarity distance (G, H) of metabolites. Values represent adjusted R^2 (%), and significance is assessed via partial db-RDA. Procrustes analysis of bacterial (E) and fungal (F) communities based on metabolic molecular structure distance and microbial phylogenetic distance. M^2 statistics represent the congruence between metabolic and microbial configurations, with *P*-values derived from permutation tests (n = 999). Redundancy analysis (RDA) illustrating the relationships between explanatory variables (metabolic bins from ICAMP analysis and soil factors) and bacterial (I) and fungal (J) community compositions. Model significance is evaluated using permutation tests (n = 999). (K) Heatmap of Z-score transformed relative abundances of metabolites within Bin 2, Bin 3, and Bin 16 across different grazing treatments. The left color bar indicates the chemical classification of root exudate metabolites, with color assignments consistent with Fig. S2. *$P < 0.05$, **$P < 0.01$, **$P < 0.001$.

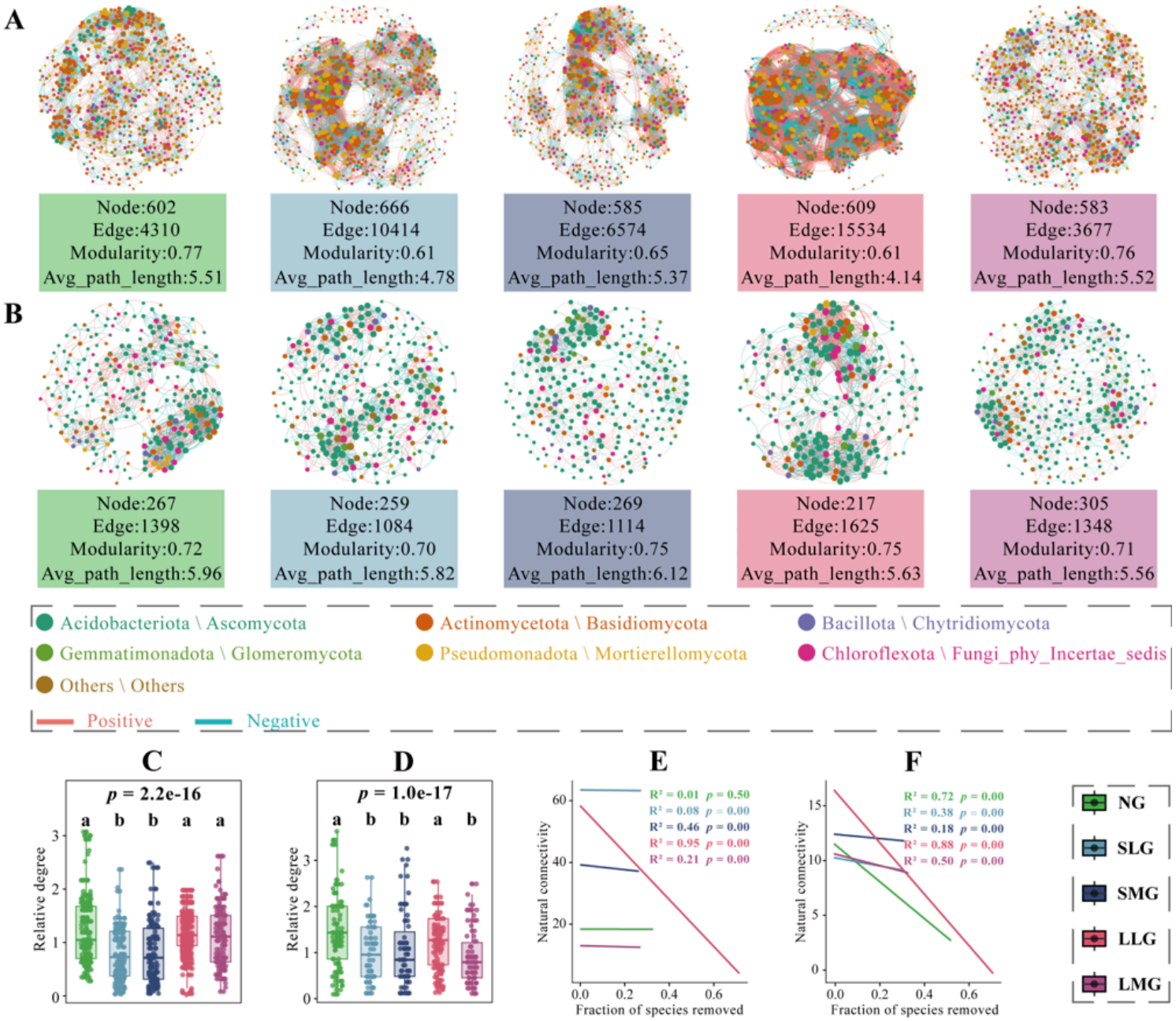

Figure 4

Fig 4. Effect of grazing on the co-occurrence network of rhizosphere microbes. Co-occurrence networks of rhizosphere bacteria (A) and fungi (B). Relative degree of bacterial (C) and fungal (D) under different grazing treatments. Differences between multiple treatments were assessed using the Kruskal-Wallis's; pairwise comparisons employed the Wilcoxon signed-rank test. Different letters indicate significant differences among treatments ($P < 0.05$). Root exudates mediate the stability of bacterial (E) and fungal (F) co-occurrence networks under different grazing treatments. The sequence of node removal for simulated extinction was determined by the mean relative degree of taxa across both the co-occurrence network and the interaction network. Linear regression of natural connectivity against the fraction of species removed, with R^2 and P values color-coded by grazing treatment.

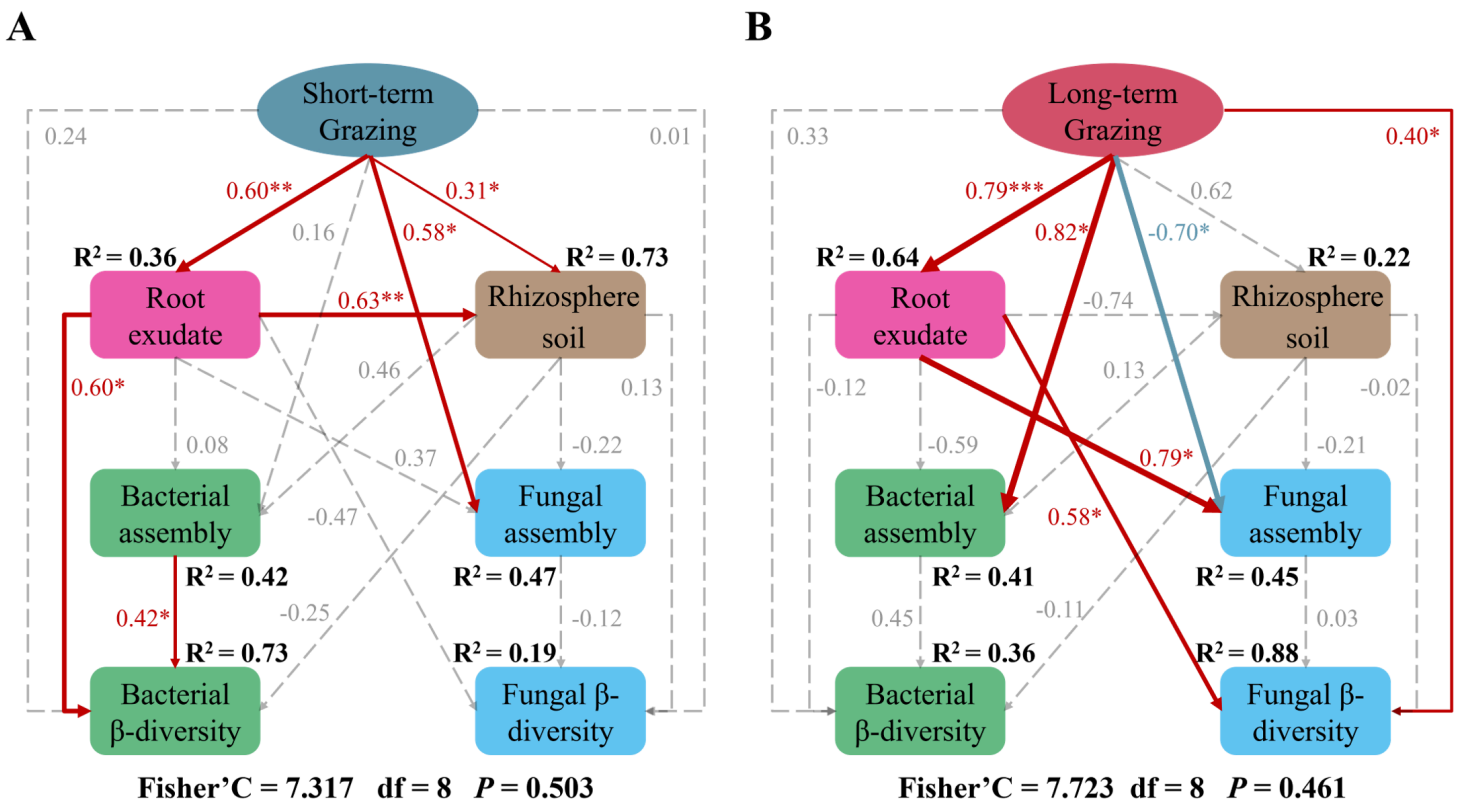

Figure 5

Fig 5. Piecewise structural equation modeling (pSEM) illustrating the direct and indirect relationships among grazing intensity, root exudate metabolites, rhizosphere soil physicochemical properties, microbial community assembly processes (dispersal limitation), and microbial community diversity under short-term (A) and long-term (B) grazing. Grazing impact was characterized by cumulative grazing pressure, calculated as the product of grazing duration and grazing intensity. Root exudate metabolites and rhizosphere soil physicochemical properties (including MC and C, N, and P-related parameters) were represented by the first principal coordinate (PCo1) derived from principal coordinate analysis (PCoA) based on Euclidean distance. Community assembly was quantified as the relative contribution of dispersal limitation. Microbial β-diversity was represented by the first axis of PCoA based on Bray–Curtis distance. Solid and dashed arrows indicate significant and not significant pathways, respectively. Red and blue arrows denote positive and negative relationships, respectively. Numbers adjacent to arrows represent standardized path coefficients, and arrow width is proportional to the strength of the relationship. R^2 values indicate the proportion of variance explained for each dependent variable. *P < 0.05, **P < 0.01, ***P< 0.001.

Supplementary Files

This is a list of supplementary files associated with this preprint. Click to download.

- file.docx